Int J Adv Manuf Technol (2008) 36:305–314
DOI 10.1007/s00170-006-0844-4

ORIGINAL ARTICLE

A new digital measurement method for accurate curve grinding process

Yong-hong Zhang · Li-hua Wang · Chun-xiang Ma · Qi Wu · De-jin Hu

Received: 28 April 2006 / Accepted: 17 October 2006 / Published online: 25 November 2006

Abstract In this paper, an online measurement and error compensation system for curve grinding based on pattern recognition was presented and verified by experiments. The measurement system organization and its principle of operation were introduced in detail. The work piece and grinding wheel image were sampled at certain positions to avoid spark influence. In order to increase system resolution, images were sampled only at local areas of the work piece and grinding wheel. A discrimination technology based on a circular tolerance zone was proposed which can solve the problem of local image edge comparison. For image de-noising, a local threshold algorithm was applied to determine new wavelet coefficients. Furthermore, a two-step edge detection method was used to realize sub-pixel precision. Finally, a series of experiments were carried out to examine the detection precision of the image measurement system and its influencing factors. From experiments, it can be said that the proposed method in this paper is effective, and its detection precision is much better than traditional methods.

Keywords Curve grinding · Pattern recognition · Circular tolerance zone · Error compensation

Y.-h. Zhang (✉) · L.-h. Wang
Department of Information and Communication,
Nanjing University of Information Science and Technology,
210044 Nanjing, China
e-mail: nuist_zyh@yahoo.com.cn

C.-x. Ma · Q. Wu · D.-j. Hu
School of Mechanical and Power Engineering,
Shanghai Jiao Tong University,
200030 Shanghai, China

1 Introduction

Grinding is commonly used as the final machining process to ensure product quality because of its high precision [1]. In recent years, high efficiency and high-performance CNC grinding machines have appeared and grinding apparatus manufacturing technology has improved. The new grinding machine has higher precision, but there is a lack of effective online detection or monitoring methods for the grinding process. Online detection plays an important role in the abrasive machining process [2].

In precision cutting tools and dies manufacturing, the final machining process is curve grinding. In this process, the grinding wheel wear will create machining errors. It is well known that the grinding wheel should be compensated when the wheel is worn out. The online measurement of grinding wheel wear and work piece is required.

At present, there are several methods for grinding wheel wear monitoring and inspection such as acoustic emission testing, hydrodynamic measurement in wet grinding, optical projection reading method, etc. [3–7]. The acoustic emission method is a dynamic nondestructive examination technology. An acoustic emission sensor is used in contact measurement to detect acoustic emission signals from the touch of the grinding wheel on a work piece. The wearing degree of the grinding wheel can be estimated by analyzing acoustic emission signals [4]. Acoustic emission signals are mainly composed of elastic contact between grinding wheel and work piece, grinding wheel binder breakage, abrasive particle breakage and work piece surface cracks, etc. It is difficult to identify the different emitters for the acoustic emission testing method [5]. Thus the grinding wheel status cannot be estimated properly.

In wet grinding, a pressure sensor was set beside the grinding wheel with a small gap. Hydrodynamic pressure,

which corresponds to the gap length and the topography, can be measured when grinding fluid was dragged into the gap by the rotation [6]. Its principle is shown in Fig. 1.

For traditional optical curve grinding machines, the grinding status estimation depended on optical projection reading. It is a non-contact, full field of vision measurement method. Its measurement principle is shown in Fig. 2. The light source was located on top of the work piece and the object lens was under the work piece. The grinding position was magnified through the optics system and focused on the display. Comparing the practical profile with the theoretical profile of work piece, the grinding status can be estimated. This method is simple and intuitionistic, but its detection precision depends on personal experience. Its detection precision is less than 10–20 μm. At the same time, this method can not collect and handle the image information; the grinding wheel wear can not be compensated timely and accurately.

With the development of charge-coupled device (CCD) and digital image processing technology, non-contact measurement online based on image analyzing appeared. An optical non-contact scanning probe consists of line laser diode and a CCD camera is placed on a computer numerical control (CNC) machine to measure the work piece profiles [7]. The measured profile data can be transferred to a CAD/CAM system for certain applications.

In order to overcome the disadvantages of traditional detection methods, a new kind of PC-based CNC system integrated with online image detection and a control system was proposed for the curve grinding process. This system can realize precision measurement, automatic compensation and in-process controlling. In this paper, an online CCD image measurement system is designed to replace the traditional optics projection reading device according to the curve grinding process. A new detection method based on the circular tolerance zone was presented. The image de-noising method based on local wavelet threshold was also introduced. Finally, the wear of the grinding wheel was compensated according to the measurement results.

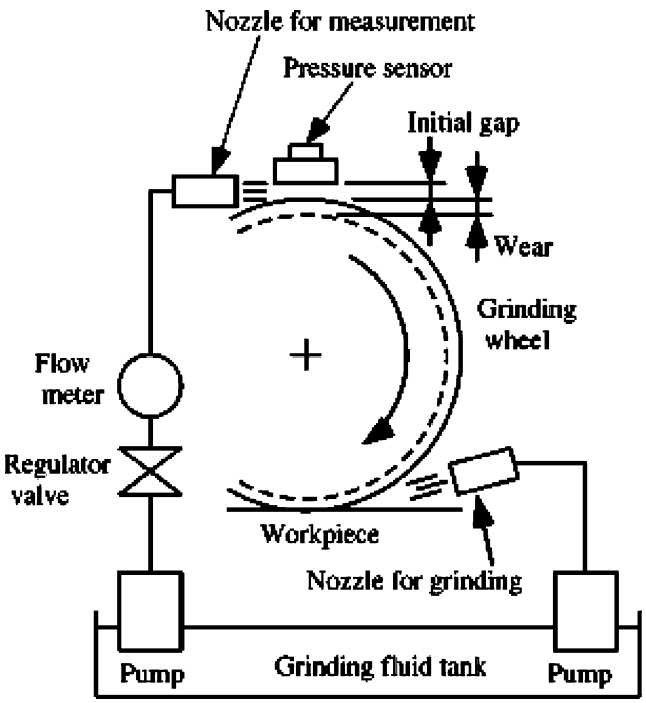

Fig. 1 Principle of measurement by using pressure [6]

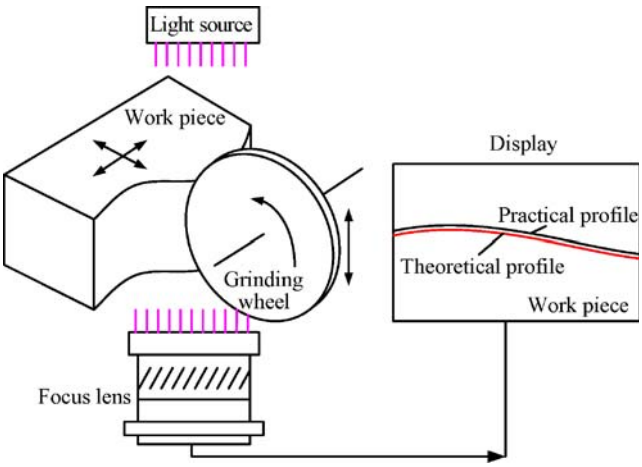

Fig. 2 Detection principle of traditional CNC optical projection profile grinding machine

2 Measurement system design and working principle

The component measurement system applied to the curve grinding process is shown in Fig. 3. The grinding wheel makes a reciprocating motion (axis-Z) in the vertical direction with high-speed rotation driven by a linear motion actuator. The work piece moves in a working table about three axes simultaneously (axes-X, Y and C). The condition

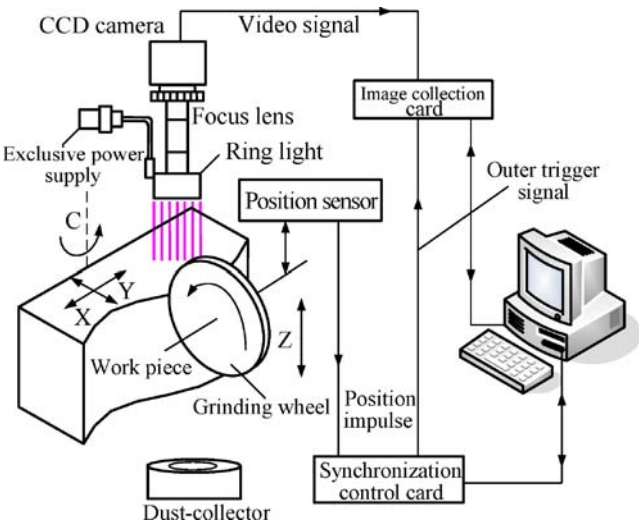

Fig. 3 Component measurement system for curve grinding

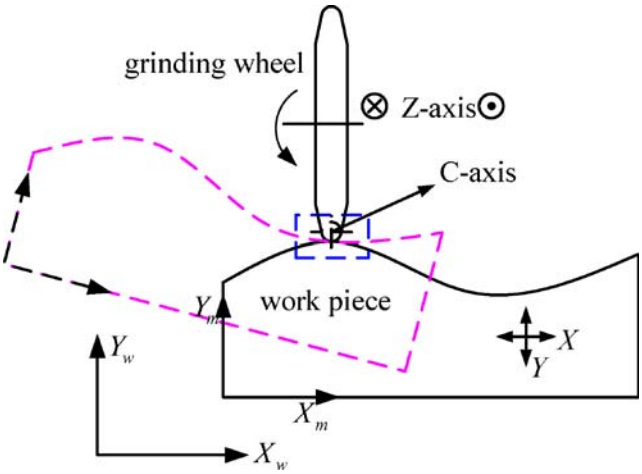

Fig. 4 Machining principle sketch of curve grinding

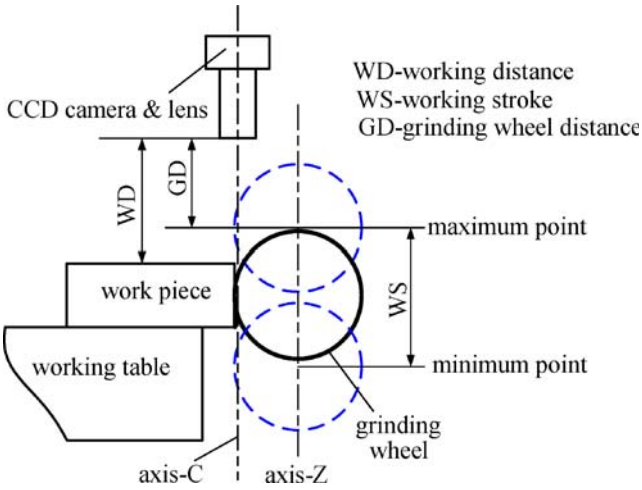

Fig. 6 The sketch of image sampling position

is dry grinding between work piece and grinding wheel. The optical imaging device consisted of the CCD camera, focus lens and ring reflected light source which are located upon the work piece and grinding wheel. Any dimensional changes in the field of CCD vision can be measured.

2.1 Curve grinding mechanism

In order to explain the principle of the measurement system, a curve grinding mechanism was introduced as shown in Fig. 4. Before curve grinding machining, the tool nose of the grinding wheel should be amended to a circular arc shape. There are three axes: the axis of the camera lens, the circular arc center of the grinding wheel nose and the rotation axis of the machine working table. These three axes should be focused on axis-C as shown in Fig. 4. Figure 5 is the magnified local area of Fig. 4. In the vertical direction as shown in Fig. 5, the grinding wheel holds still. The work piece moves in the working table along the axis-X and axis-Y, and at the same time it moves around axis-C. Thus the complex curve profile can be determined. The normal direction at the work piece grinding point is coinciding with the grinding wheel normal direction.

2.2 Object image sampling

The main process of the whole measurement system for object image sampling can be expressed as follows.

Firstly, there are sparks during machining because of dry grinding. These sparks may largely influence image sampling of work piece and grinding wheel. So the image sampling should occur at a certain position where there isn't any spark. Figure 6 gives a sketch of the image sampling position. As we know, there isn't any spark when the grinding wheel moves at the maximum point; therefore, at this moment, the sampled image of work piece and grinding wheel is not influenced by sparks.

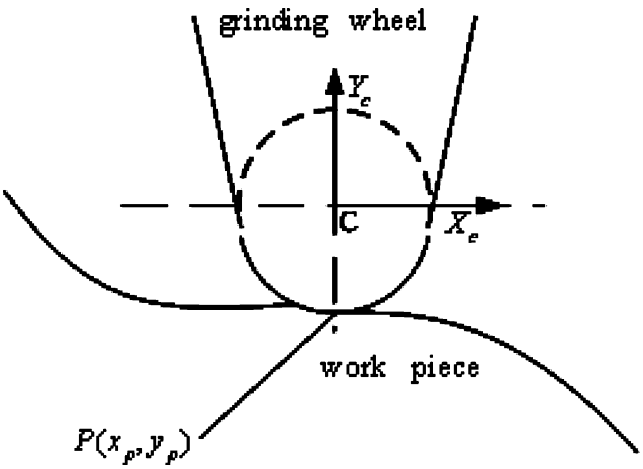

Fig. 5 The relationship between grinding wheel and work piece at grinding point

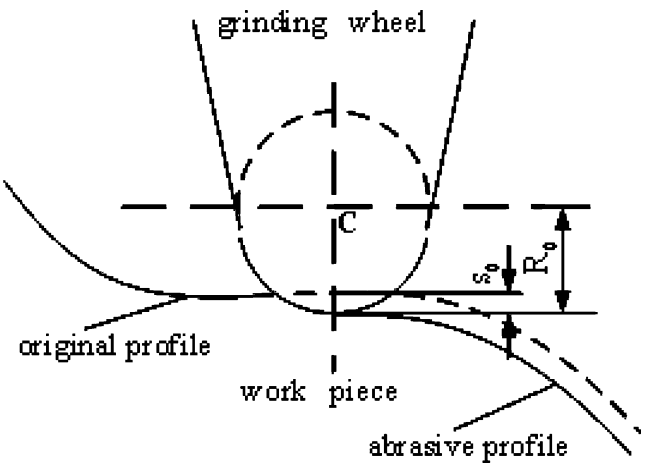

Fig. 7 Sketch of grinding wheel without wear

Secondly, it can be seen that the position sensor checks grinding wheel motion (Fig. 3), and its position impulse was detected by a synchronization control card. In order to avoid sparks influence, when the synchronization control card detects the position impulse of the grinding wheel at the maximum point, the synchronization control card will emit a short-time current impulse signal to trigger image collection card sampling of the work piece and grinding wheel. The debris seldom affects the quality of the image because spark was avoided at the sampling position and the dust-collector is always working during machining.

Finally, sampled images of the work piece and grinding wheel were saved in the computer. Physical dimensions of the work piece and grinding wheel can be examined by applying image processing software while the CCD camera is calibrated. Grinding wheel wear can be compensated by the CNC system according to the measurement results.

2.3 Measurement method based on circular tolerance zone

Abrasive machining is a slow wear process for the grinding wheel. s_0 is the commanded feeding allowance. If the measured feeding allowance equals s_0 as shown in Fig. 7, then there is no error and the grinding wheel is not worn out. If grinding wheel wear occurs, as shown in Fig. 8, the measured allowance s is less than s_0, and the wear can be determined by Eq. 1.

$$w = s_0 - s = R_0 - R \tag{1}$$

Here w is the wear rate of the grinding wheel, and R_0 and R are the circular arc radius of the grinding wheel before and after wear occurs, respectively.

But there are some problems with this method. The sampled image of the grinding wheel is usually blurred. The detected image edge is not accurate. As is well known, the surface of the grinding wheel is composed of small abrasive particles. During optical imaging, it is easy to cause diffuse reflection because of small abrasive particles, and the image edge of the grinding wheel is blurred. If the commanded feeding rate s_0 of the grinding wheel is too small, this method can hardly detect the wear of the grinding wheel. Thus, it is unsuitable to detect grinding wheel wear in the curve grinding process. The detection object should be the work piece.

In image measurement, if the resolution of the CCD camera is definitive, the measuring precision decreases with increasing size of the CCD camera field of view. In general conditions, the work piece is much lager than the CCD camera field of view. That is to say, the sampled image is only a part of the work piece. As shown in Fig. 5, the grinding error of the work piece can be obtained by comparing the practical abrasive profile with the theoretical abrasive profile. But it is difficult to guarantee that the coordinates of the practical abrasive profile correspond to those of the theoretical abrasive profile. Here a detection method based on circular tolerance zone is presented.

The detection principle of the circular tolerance zone method is shown in Fig. 9. It is an idealized statement supposing a grinding wheel without any wear. Here s_0 is the commanded feeding rate. If there isn't any wear for the grinding wheel, the practical abrasive profile is the theoretical profile as shown in Fig. 9. In fact, the grinding wheel will certainly wear during machining. The work piece is acceptable if the deviation between the practical abrasive profile and the theoretical abrasive profile is less than a scheduled tolerance. Here the scheduled tolerance is named ε shown in Fig. 9. The tolerance zone is a strip area along the theoretical abrasive profile. During the grinding process, the work piece moves in a horizontal plane by three-axis simultaneous motion (axes-X, Y and C). The

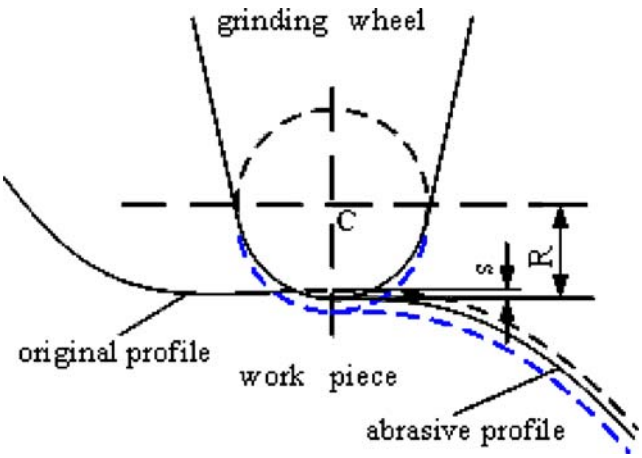

Fig. 8 Sketch of grinding wheel with wear

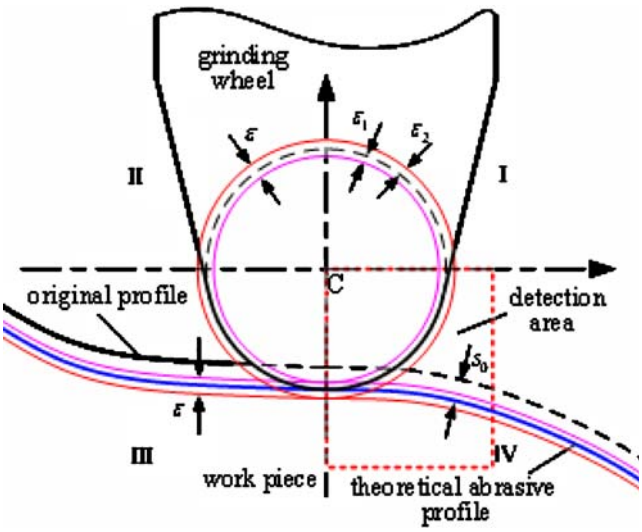

Fig. 9 Detection principle of circular tolerance zone

theoretical abrasive profile, the practical abrasive profile and the strip tolerance zone are always changing while the work piece is moving. So it is difficult to compare the theoretical with the practical profile. As presented, the tool nose of the grinding wheel should be amended as a circular arc. This circular arc corresponds to the theoretical abrasive profile of the strip tolerance zone. But this theoretical circular profile of the grinding wheel is stationary from the view orientation of the CCD camera. So the strip tolerance zone ε can be converted into a circular tolerance zone. Here

$$\varepsilon = \varepsilon_1 + \varepsilon_2 \tag{2}$$

Here ε_1 is named inner deviation and ε_2 is named outer deviation. There are parts of the original profile and abrasive profile of the work piece in the circular zone area as shown in Fig. 9. The practical abrasive profile is located in the 4th quadrant area. So the detection area can be determined as shown in Fig. 9.

The acceptable status of curve grinding was shown in Fig. 10. The work piece is considered acceptable if there are parts of the practical abrasive profile locating in the circular tolerance zone at the detection area. At the same time, there isn't any practical abrasive profile locating in the area of outer ε_1. That is to say, the curve grinding machining may continue at this status and needn't compensate the grinding wheel wear.

Figure 11 shows the status of the worn-out grinding wheel. The grinding wheel is considered worn out if there are parts of the practical abrasive profile locating in the area of outer ε_1 as shown in Fig. 11. At this moment, the detection result is fed back to CNC system. The grinding wheel should be compensated at a predefined rate.

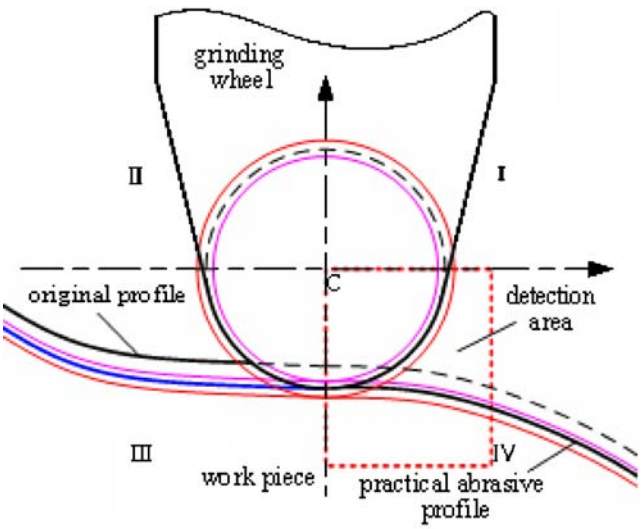

Fig. 10 Acceptable status of curve grinding

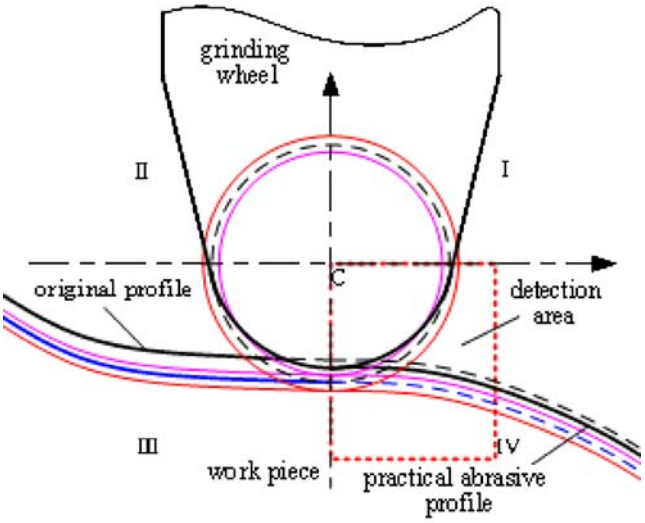

Fig. 11 Status of worn-out grinding wheel

3 Digital image processing

3.1 Local wavelet threshold for image de-noising

Images are often contaminated by noise in their acquisition, by transmission as well as the vibration of machine tools during the curve grinding process. In order to reduce the noise and retain the important signal features, traditional de-noising methods have been applied by linear processing, such as Wiener filtering. But the traditional method smooths the image edge while de-noising.

Recently, wavelet transformation has been widely used in image de-noising [8]. In this paper a wavelet local threshold method was adopted for image de-noising. Its main procedures can be expressed as follows. Firstly, two-dimension discrete wavelet transform was applied to the noised images. Secondly, wavelet coefficients were disposed by threshold selection. Here a kind of wavelet threshold function with the characteristics of continuous and derivatives was presented [9, 10]. The third step was choosing thresholds. A local threshold algorithm was used to compute different scale thresholds, another threshold was suggested when there is minimum mean-square error. The final thresholds were determined after comparing the upper two thresholds. Finally, image signals were reconstructed through invert discrete wavelet transform with the new wavelet coefficients, and then the de-noised image can be obtained.

3.2 Sub-pixel edge detection

The image edge detection precision is very important for this measurement system according to its working princi-

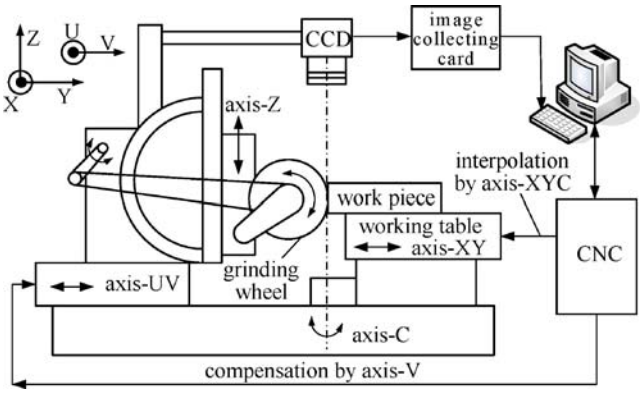

Fig. 12 System configuration for automatic compensation based on image measurement

ple. As is known, there are some traditional edge detection operators such as Robert, Sobel, Prewitt, Canny, etc. Their detection precision is limited at a certain CCD camera resolution and measurement field of view. The edge localization precision of these traditional operators is only one-pixel.

In order to improve the edge localization precision, here a sub-pixel edge detection operator based on spatial moment operator was used [11]. Firstly, the image edge was localized using Laplacian of Gaussian (LOG) because of its high efficiency. And one-pixel level edges can be obtained. Secondly, applying the sub-pixel edge operator to the neighborhood of edge beside edge points, the high precision edge localization can be realized [12].

4 Automatic compensation of grinding wheel wear

The measurement system principle has already been introduced in this paper. When the sampled images of the work piece were written into the computer, the grinding status can be examined by applying the image process software. If the grinding wheel is worn out, the computer transfers compensation commands as well as NC commands to the grinding machine. The CNC servo system controls axis-V of the grinding machine to complete the compensation feeding as shown in Fig. 12.

Fig. 13 MD9040 digital curve grinding machine

Table 1 Main technical parameters of MD9040

Subject	Quantity/Measurement
Number of control axes	6
CCD detection precision	2 μm
Field of view	12 mm×8 mm
Working distance (WD)	120 mm
Reciprocating distance of slider	2 mm–150 mm
Reciprocating times of slider	0–300 min^{-1}
Machining surface roughness (Ra)	0.32 μm
Min. input increment of CNC	0.1 μm

5 Experimental studies and conclusions

5.1 Experimental setup

Experiments were done on an MD9040 digital curve grinding machine as shown in Fig. 13. This grinding

Table 2 Specifications of image sampling instruments

		Specification
CCD camera	Camera model	COSTAR SI-M350
	CCD sensor	1/2″ Hyper HAD IT CCD
	Effective no. of pixels	752(H)×582(V)
	Scanning area (mm)	6.45(H)×4.84(V)
	Resolution	H: 570 TV lines V: 480 TV lines
	Shutter	0–1/400,000
Camera lens	Model no.	Computar TEC-M55
	Focal length	55 mm
	Max. aperture ratio	1:2.8
	Object distance	100 mm–5000 mm
	Mount	C-Mount
Focus lens		Computar TEC-M55
Synch. control card		DANFOSS
Light source		OSe RIN-70-3R-0R
Image collecting card		PXC200A external trigger; Resolution: 640×480

Fig. 14 The practical image sampling system

machine is a multi-functional machine with online image measurement, automatic compensation, and open multi-simultaneous control. Table 1 shows the specifications of this grinding machine. WD means the distance between work piece and camera lens.

Table 2 shows the specifications of the CCD image measurement instruments used in the experiment. The magnification of the measurement system is M=0.5. For the CCD camera, the output number of pixels is 739 (H)×575(V), and its effective ratio is 0.983×0.988. So the measurement fields of view along directions X and Y are:

$$FOV\_X = 6.45 \times 0.983/0.5 = 12.6807\,\text{mm} \quad (3)$$

$$FOV\_Y = 4.84 \times 0.988/0.5 = 9.5638\,\text{mm} \quad (4)$$

The image collection card is PXC200A of CyberOptics Corp. Its resolution is 640×480. So the resolutions of the whole measurement system along directions X and Y are:

$$R\_X = 12.6807/640 = 0.01981\,\text{mm} = 19.81\,\mu\text{m} \quad (5)$$

$$R\_Y = 9.5638/480 = 0.01992\,\text{mm} = 19.92\,\mu\text{m} \quad (6)$$

In the Table 1, the requirement of CCD detection precision is 2 μm. If using the traditional image edge

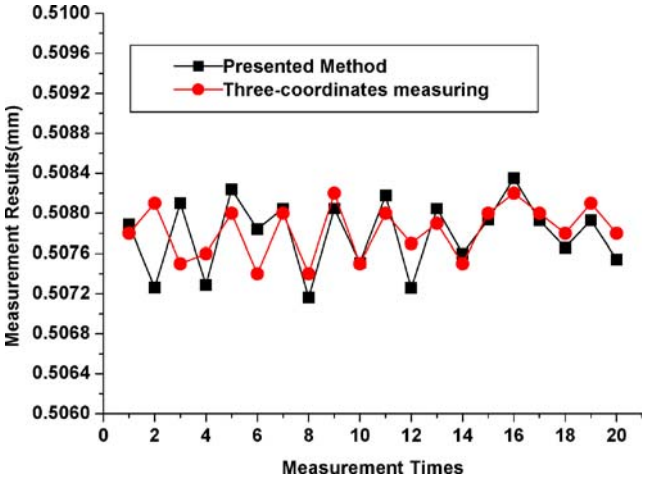

Fig. 15 Offline detection results

detection operators, the image edge localization precision is only about 20 μm (Eqs. 5 and 6).

5.2 Measurement results and precision analysis

In order to estimate the detection precision of the image measurement system and its influencing factors, a series of experiments were done. Figure 14 is the practical image sampling system.

The CCD camera should be calibrated firstly before detection. The calibration template is manufactured by Alpen Technology Corp. In order to improve calibration precision, an equivalent diameter demarcate approach was used. The result of calibration is 0.0162944 mm/pixel.

The first experiment was offline detection. The stated grinding feed rate is L_0=0.508 mm in the experiment. Measurement began after grinding was finished, and the grinding environment light intensity is stationary. The measurement results are shown in Fig. 15. The results were not influenced by machining vibration because of offline

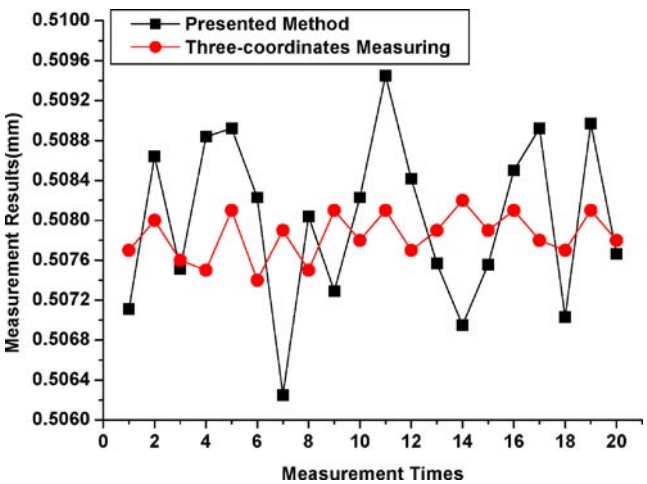

Fig. 16 Online detection results

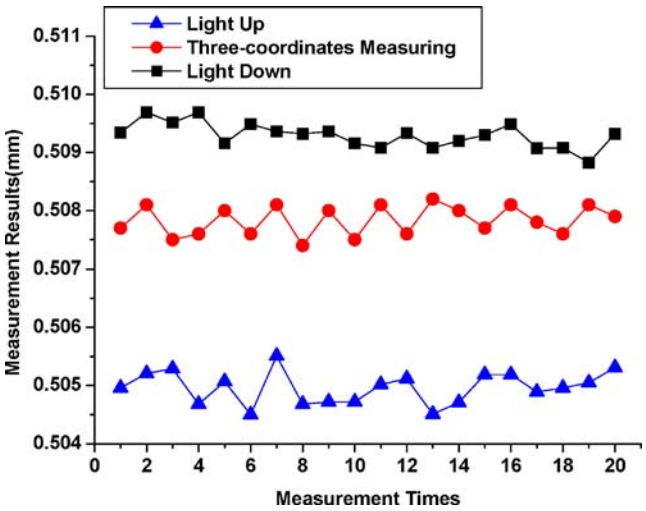

Fig. 17 Influence of light source

detection, and the measurement results reflect the image edge detection precision as shown in Fig. 15.

For the presented method,

$$L_{\max} = 0.5084\,\text{mm},\ L_{\min} = 0.5072\,\text{mm}$$

Its measurement error is

$$\Delta E = \max\{|L_{\max} - L_0|, |L_{\min} - L_0|\} = 0.8\,\mu\text{m}$$

For three-coordinate measuring,

$$L_{\max} = 0.5082\,\text{mm},\ L_{\min} = 0.5074\,\text{mm}$$

Its measurement error is

$$\Delta E = \max\{|L_{\max} - L_0|, |L_{\min} - L_0|\} = 0.6\,\mu\text{m}$$

From the measurement results, it can be seen that the system has high detection precision applying the sub-pixel edge localization operator.

The second experiment was online detection. In this experiment the stated grinding feed rate is also L_0= 0.508 mm. In order to reduce the influence of machining vibration, the system filtered vibration frequency during measurement processing. Figure 16 gives the measurement results of online detection.

For the presented method,

$$L_{\max} = 0.5094\,\text{mm},\ L_{\min} = 0.5062\,\text{mm}$$

Its measurement error is

$$\Delta E = \max\{|L_{\max} - L_0|, |L_{\min} - L_0| = 1.8\,\mu\text{m}\}$$

For three-coordinate measuring,

$$L_{\max} = 0.5082\,\text{mm},\ L_{\min} = 0.5074\,\text{mm}$$

Its measurement error is

$$\Delta E = \max\{|L_{\max} - L_0|, |L_{\min} - L_0|\} = 0.6\,\mu\text{m}$$

Fig. 18 Setting interface of the measurement system. **a** Display area of work piece and grinding wheel imaging. **b** Display area of machine coordinates. **c** Operation buttons for user. **d** Setting area of image sampling

Fig. 19 The instant image during curve grinding. **a** Display area of work piece and grinding wheel imaging. **b** Display area of machine coordinates. **c** Operation buttons for user. **e** Display area of NC codes

From the measurement results, it can be seen that there are some influences due to machining vibration. But the system still has high detection precision of less than 2 μm.

The third experiment is to test the influence of the light source. In the upper two experiments, the light source intensity was stationary. The detection results will be influenced by changing light source intensity after calibration. In this experiment, the working conditions were equal to the upper experiments. The detection results are shown in Fig. 17.

It can be seen that the detection results became larger while reducing light intensity and became less while increasing light

Fig. 20 The instant interface of the measurement system. **a** Display area of work piece and grinding wheel imaging. **b** Display area of machine coordinates. **c** Operation buttons for user. **f** The instant interface of detection results

intensity. These changes are transparent. The image edge was sharpened while increasing light intensity and detection results will become less. Inversely, the results will become larger. The light changing will largely influence detection results. In the practical detection, the light intensity should be stationary.

5.3 Practical detection of the curve grinding process

The purpose of these experiments was to verify the system detection precision. It does not present the practical grinding status. For the practical detection of the curve grinding process, here the experiment was done to inspect its validity. Before the practical curve grinding, the measurement system should be settled according to the thickness of the work piece and processing techniques. In this experiment as shown in Fig. 18, the maximum point was set as 80 mm, and the minimum point at 20 mm. The image sampling point was set as 60 mm, and the reciprocate speed of grinding wheel was 240 mm/s.

The intersection point of the red cross-hairs was just the rotation center of axis-C as shown in Fig. 18. Before the curve grinding process, the circular arc center of the grinding wheel and the rotation center of the machine working table should be focused on the intersection point of the red cross-hairs. The red endless belt is the circular tolerance zone. As mentioned in Sect. 2.3, the measurement system differentiates whether the practical abrasive profile of the work piece is located in the area of circular tolerance zone.

During the curve grinding process, the grinding wheel reciprocates in the vertical direction. As is well known, the profile of a grinding wheel may be located in the area of the circular tolerance zone during processing if the image of the grinding wheel has a clear edge profile as shown in Fig. 19. The measurement system may inform some compensation alarms. The measurement system was used to detect whether the edge profile of the work piece was located in the area of the circular tolerance zone. So the image of the grinding wheel and work piece should be separated. In the experiment, the CCD camera can sample clear images of the grinding wheel at Z=40. In order to avoid the problem just described, the sampling position was set at Z=60, as shown in Fig. 18. At this moment, in the sampled image of work piece and grinding wheel, the work piece was clear and the grinding wheel was blurry. For this sampled image, the binarization method was applied and the blurred image of the grinding wheel can be filtered as shown in Fig. 20. Then the edge profile of the work piece can be estimated based on the circular tolerance zone technology. The instant interface of the measurement system is shown in Fig. 20.

In conclusion, the measurement method presented in this paper is a new technology for the curve grinding process. This method has high detection precision and was successfully used in curve grinding detection and automatic compensation. From the experiments described, it can be seen that there are many factors which affect the image quality and the results of image processing, especially in real machining. In the future work, further investigation and research are still needed in such topics as machine tool vibration, light strength and direction.

Acknowledgement The authors would like to thank Shanghai No.3 Machine Tool Factory for the joint research. This work was supported by the Foundation of Shanghai Science and Technology Committee (No.021111125) and the Foundation of Nanjing University of Information Science and Technology.

References

1. Fan KC, Lee MZ, Mou JI (2002) On-line non-contact system for grinding wheel wear measurement. Int J Adv Manuf Technol 19:14–22
2. Tonshoff HK, Friemuth T, Becker JC (2002) Process monitoring in grinding. Ann CIRP 51(2):551–571
3. Kim H, Kim SR, Ahn JH (2001) Process monitoring of center less grinding using acoustic emission. J Mater Process Technol 111:(1–3)273–278
4. Wang Z, Willett P, Deaguiar PR (2001) Neural network detection of grinding burn from acoustic emission. J Mach Tools Manuf 41(2):283–309
5. Pawel K (2001) An intelligent system for grinding wheel condition monitoring. J Mater Process Technol 109(3):258–263
6. Furutani K, Hieu NT, Ohguro N, Nakamura T (2003) Automatic compensation for grinding wheel wear by pressure based in-process measurement in wet grinding. Precis Eng 27:9–13
7. Chang M, Liu KH (1999) Non-contact scanning measurement utilizing a space mapping method. Opt Lasers Eng 30:503–512
8. Mallat S, Zhong S (1992) Characterization of signals from multi-scale edges. IEEE T Pattern Anal 14(7):710–732
9. Donoho DL (1995) De-noising by soft-threshold. IEEE T Inform Theory 41(3)613–627
10. Chang SG, Yu B, Vetterli M (2000) Adaptive wavelet thresholding for image de-noising and compression. IEEE T Image Process 9(9):1532–1546
11. Lyvers EP, Mitchell OR (1989) Sub-pixel measurements using a moment based edge operator. IEEE T Pattern Anal 11(12):1293–1309
12. Zhang Y, Hu D, Xu J (2004) Subpixel edge location of machine parts based on the vision images. Chi Hsieh Kung Ch'eng Hsueh Pao 40(6):179–182 (in Chinese)